C-H Activation and Proton Transfer Initiate Alkene Metathesis Activity of Tungsten (IV)-Oxo Complex

Ka Wing Chan[†], Erwin Lam[†], Vincenza D'Anna[‡], Florian Allouche[†], Carine Michel[‡], Olga V. Safonova[§], Philippe Sautet[‡,&,ç], Christophe Copéret*[,†]

[†] ETH Zürich, Department of Chemistry and Applied Biosciences, Vladimir Prelog Weg 1-5, ETH Zürich, CH-8093 Zurich, Switzerland

[‡] Univ Lyon, Ens de Lyon, CNRS UMR 5182, Université Claude Bernard Lyon 1, Laboratoire de Chimie, F-69342, Lyon, France

[§] Paul Scherrer Institute, CH-5232 Villigen, Switzerland

[&] Department of Chemical and Biomolecular Engineering, University of California, Los Angeles, Los Angeles, California 90095, United States

[ç] Department of Chemistry and Biochemistry, University of California, Los Angeles, Los Angeles, California 90095, United States

ABSTRACT: In alkene metathesis, while group 6 (Mo or W) high-oxidation state alkylidenes are accepted to be key reaction intermediates for both homogeneous and heterogeneous catalysts, it has been proposed that low valent species in their +4 oxidation state can serve as pre-catalysts. However, the activation mechanism for these latter species – generating alkylidenes – is still an open question. Here, we report the syntheses of tungsten (IV)-oxo bisalkoxide molecular complexes stabilized by pyridine ligands, $WO(OR)_2py_3$ (R = $CMe(CF_3)_2$ (**2a**), R = $Si(OtBu)_3$ (**2b**) and R = $C(CF_3)_3$ (**2c**); py = pyridine) and show that upon activation with $B(C_6F_5)_3$, they display comparable alkene metathesis activities as W(VI)-oxo alkylidenes. The initiation mechanism is examined by kinetic, isotope labeling and computational studies. Experimental evidence reveals that the presence of an allylic CH group in the alkene reactant is crucial for initiating alkene metathesis. Deuterium-labeling of the allylic C-H group shows a primary kinetic isotope effect on the rate of initiation. DFT calculations support the formation of an allyl hydride intermediate via activation of the allylic C-H bond and show that formation of the metallacyclobutane from the allyl "hydride" involves a proton transfer facilitated by the coordination of a Lewis acid ($B(C_6F_5)_3$) and assisted by a Lewis base (pyridine). This proton transfer step is rate determining and yields the metathesis active species.

INTRODUCTION

Alkene metathesis is increasingly impacting different fields of chemistry, ranging from petrochemical to pharmaceutical industries.[1-13] Today, the largest industrial alkene metathesis process is based on WO_3/SiO_2, a heterogeneous catalyst, which only operates at high temperatures (> 400 °C).[14] Pre-treating this catalyst under reducing conditions (e.g. alkene, H_2 etc.) allows the process to be operated at lower temperatures, thus indicating that the high temperature conditions are mostly needed for generating the active sites.[15-19] Similar pre-treatment effect has also been reported for supported Mo based catalysts.[20-22] Recently, our group has reported a low temperature activation method based on organosilicon reductants, which allow MO_3/SiO_2 (M = Mo or W) and the related well-defined silica-supported metal-oxo species to catalyze alkene metathesis at 70 °C. We have proposed that M(IV) species bearing an oxo ligand, which are formed upon reduction, can transform into alkylidene species in the presence of alkenes.[23-24] Previous works in homogeneous catalysis have shown that Mo(IV)(NAr)(X)(Y)(alkene) and dimeric $\{W(NAr')[OCMe_2(CF_3)]_2\}_2$ complexes (Scheme 1), which can be formed from the alkylidenes during metathesis, can also re-initiate metathesis, albeit with a very low efficiency.[25-26] In fact, the numbers of active species generated under these conditions have been reported to be very small (< 3%).

Scheme 1. Transformation of M(IV) pre-catalysts to active M(VI) alkene metathesis catalysts

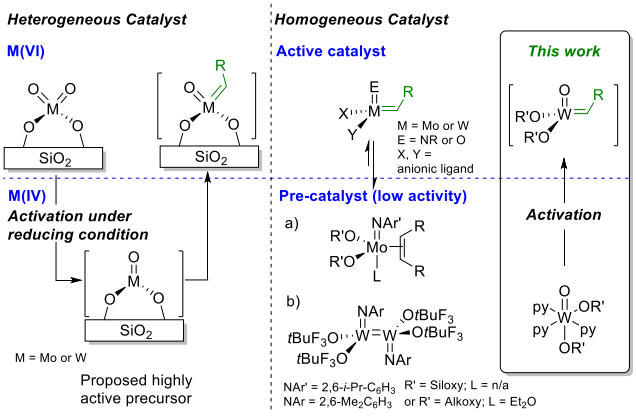

Thus, understanding how alkylidenes can be regenerated in-situ from M(IV) molecular species would be valuable as it could help to design methods for reactivation and ways to improve overall catalysts performance.[8] In view of the reported metathesis activities of reduced group 6 metal sites in homogeneous systems and the high activities of the putative W(IV)-oxo sites in supported systems, we reason that molecu-

lar W(IV) complexes bearing oxo and alkoxide ligands would be an ideal system to probe the initiation step and a source of potentially efficient catalyst precursors.

There are only few W(IV)-oxo complexes known: i) $WOCl_2(PX_3)_3$ (PX_3 = $P(OMe)_3$, PMe_2Ph, $PMePh_2$)[27-28], which can react with strained cyclopropenes to form metathesis active vinylalkylidenes and ii) $WO(OR)_2$(alkene) (OR = 2,6-dimesitylphenoxide or 2,6 -diadamantyl-4-methylphenoxide), which can be formed upon decomposition of the corresponding alkylidenes, but which has not been reported to engage in alkene metathesis.[29] Here, we report the preparation of monomeric d^2 W(IV)-oxo complexes bearing electron-withdrawing alkoxide and stabilizing pyridine ligands; they show high activities in metathesis upon activation with $B(C_6F_5)_3$. We show by using a combined experimental and computational approach that the activation mechanism for initiating alkene metathesis and formation of alkylidene involves two key steps: i) the C-H bond activation of an allylic C-H group that must be present in the alkene reactant, and ii) a proton transfer process facilitated by pyridine and $B(C_6F_5)_3$.

RESULTS AND DISCUSSION

W(VI)-oxo complexes $WOCl_2(OR)_2L$ (**1a**: R = $CMe(CF_3)_2$ = *t*BuF_6 and L = pyridine = py, **1b**: R = $Si(OtBu)_3$ and L = Et_2O) were synthesized by salt metathesis of $WOCl_4$ and 2 equiv of LiOR in diethyl ether (Scheme 2). The pure products were obtained as colorless crystals in ca. 70% yield upon recrystallization in pentane at –40 °C. The alkoxide groups are *trans* to each other according to NMR spectroscopies and single crystal X-ray diffraction studies (see SI).

Scheme 2. Synthetic routes for complexes 1a-1b, 2a-2c and X-ray crystal structure of 2b[a]

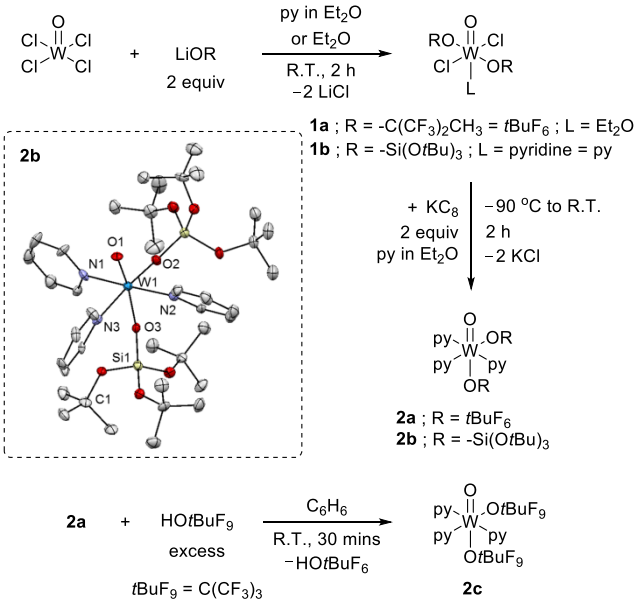

[a]Thermal ellipsoids plot at 50% probability; hydrogen atoms omitted.

The subsequent reduction of these compounds with KC_8 at –90 °C in the presence of pyridine yields their W(IV) analogues $WO(OR)_2py_3$ (**2a** and **2b**), which can be obtained as dark blue crystals after recrystallization in pentane at –40 °C. Attempts of using the same synthetic route to synthesize $WO(OC(CF_3)_3)_2py_3$ (**2c**) resulted in a mixture of products. However, pure **2c** could be obtained as pure dark purple solid from protonolysis of **2b** with perfluoro-*tert*-butanol (Scheme 2), similar to the reaction of pyrrole complexes with various alcohols.[30] We have so far not been able to prepare the corresponding O*t*Bu or $OC(CH_3)_2(CF_3)$ complex by the approaches described above. The three six-coordinated octahedral $WO(OR)_2py_3$ complexes described above are diamagnetic and share the same geometry with one of the OR groups on the equatorial plane and the other one at the axial position *trans* to the oxo ligand (see SI, Figure S2-4). Attempts to use other weakly coordinating ligands instead of pyridine, such as THF or dimethoxyethane, did not yield any desirable product.

Reaction of the complex **2a** with *cis*-4-nonene (300 equiv/[W]) shows no activity in metathesis at 70 °C, even after 24 h. This can be ascribed to the absence of an empty coordination site due to the relative strong binding of pyridine in these complexes.[31] On the other hand, in the presence of a Lewis acid, such as $ZnCl_2$(dioxane) or $B(C_6F_5)_3$, metathesis activity is observed, presumably due to the removal of pyridine. While equilibrium conversion is not reached with $ZnCl_2$(dioxane) (3 equiv/[W]) after 24 h (Figure S7), 3 equiv of $B(C_6F_5)_3$ leads to equilibrium conversion (51%) of *cis*-4-nonene (300 equiv/[W]) within 12 h at 70 °C. The catalytic activities of complexes **2a-2c** in the presence of $B(C_6F_5)_3$ are shown in Table 1.

Table 1. Catalytic activities of complexes 2a-2c.[a]

Catalyst precursor	*Loading /mol %*	*$B(C_6F_5)_3$ /mol%*	*Substrate*	*TOF[c] /min^{-1}*	*Equil. Time[d]*
2a	0.3	1	4-nonene[b]	2	12 h
	0.3	1.3	4-nonene[b]	4	3 h
2b	0.3	1	4-nonene[b]	2	12 h
2c	0.3	1	4-nonene[b]	15	0.5 h
	0.3	1.3	4-nonene[b]	11	0.5 h
	1	3	1-nonene	7	83%$^{24\ h}$

[a]1.0 M toluene solution, batch reactor, 70 °C; [b]*cis*-4-nonene; [c]TOF is expressed as initial TOF after 3 min of reaction; [d]Time to reach equilibrium conversion unless otherwise noted by giving the final conversion after 24 h.

Similar activities are observed for the hexafluoro-*tert*-butoxide (**2a**) and siloxide complexes (**2b**), but the perfluoro-*tert*-butoxide complex (**2c**) shows a significantly higher activity (time to equilibrium < 30 min). These activities are comparable to those reported for the corresponding pre-formed molecular W-oxo alkylidene complexes.[32-36] With the terminal alkene 1-nonene, the initial activity is similar to that of internal *cis*-4-nonene, but a significantly higher catalyst loading (1 mol% catalyst) is required to reach 83 % conversion. Increasing the amount of $B(C_6F_5)_3$ (4 equiv/[W]) further increases the catalytic activity of complex **2a** and reduces the time to reach equilibrium conversion from 12 h to 3 h, while this approach has little to no effect on **2c**.

Encouraged by the promising catalytic results, we further studied the activation mechanism involved in transforming these W(IV)-oxo species into W(VI)-oxo alkylidenes. Several activation mechanisms have been proposed for the formation of active M(VI) (M = Mo or W) alkylidenes from M(IV) precatalysts (Scheme 3).[26, 37] The first possibility involves the formation of a metallacyclopentane, which can subsequently undergo ring contraction via β-H transfer followed by an insertion to yield a metallacylcobutane that can participate in metathesis.[38-39] Alternatively, the second and third pathways require a vinyl and an allylic C-H activation, respectively. The fourth pathway involves a dimeric species, which has been

proposed to undergo [2+2] cycloaddition with reactive olefins (norbonene or diallylether).[25] Since one of the mechanisms should be specific to alkene containing the allylic CH group, we first set to investigate the reactivity of complex **2a** towards alkenes with or without allylic CH groups.

Scheme 3. Proposed oxidative initiation mechanisms

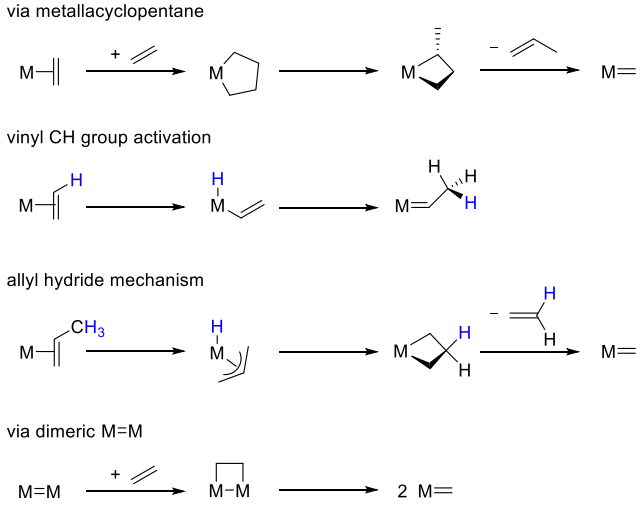

Reaction of **2a** in C_6D_6 with ethylene leads to an immediate color change from dark blue to yellow at room temperature. By in-situ ^{1}H-NMR, free pyridine and new proton signals at δ 3.04 and 2.84 ppm are observed. In the ^{13}C-NMR spectrum, a characteristic singlet peak is observed at δ 65.3 ppm (J_{WC} = 22.9 Hz) indicating the formation of ethylene π complex, **3a-C_2H_4** (Scheme 4).[26, 40] **3a-C_2H_4** can be isolated by recrystallization in toluene at –40 °C and its structure is confirmed by single crystal X-ray diffraction studies. The C1=C2 bond distance of the coordinated ethylene molecule is 1.41 Å, indicating a significant back donation from the metal center to the π^* orbital of ethylene.[41] In the presence of 3 equiv of $B(C_6F_5)_3$, the reaction of **2a** and ^{13}C-dilabeled ethylene yields the py-$B(C_6F_5)_3$ adduct, **3a-C_2H_4** along with a small amount of the metallacyclopentane **4a** (Scheme 4) at room temperature. Heating the reaction mixture to 50 °C leads to complete conversion of **3a-C_2H_4**, removal of most of the coordinated pyridine from W centers to give py-$B(C_6F_5)_3$ (ca. 3 equiv/[W]) and increases the amount of **4a**. The complex **4a** gives rise to two broad peaks at ca. δ 3.0 ppm and 2.8 ppm in the ^{1}H-NMR spectrum. These signals correlate with the carbon resonances at δ 74.8 (α-C) and 36.4 ppm (β-C), respectively, in the ^{13}C-NMR spectrum according to ^{1}H-^{13}C HSQC experiment (Figure S10-S12). These resonances are similar to those reported for other metallacyclopentane complexes of Mo and W.[26, 29, 40-43] No peak associated with the metallacyclobutane or alkylidene is observed in ^{1}H and ^{13}C NMR, even upon further heating at 70 °C. While a small amount of 1-butene is observed, likely resulting from the decomposition of **4a** after prolonged heating (Figure S10), this process seems to be relatively slow. The rearrangement of metallacyclopentane to 1-butene has also been reported in several high valent metallacyclopentane complexes.[26, 40, 42, 44] The complex **4a** slowly decomposes under high vacuum (10^{-5} mbar) or in the absence of ethylene making its isolation unsuccessful so far. The absence of metallacyclobutane may also suggest that **4a** does not undergo ring contraction readily (Scheme 3; first pathway).

Scheme 4. Reaction of 2a with ethylene in the presence of $B(C_6F_5)_3$ and X-ray crystal structure of 3a-C_2H_4[a]

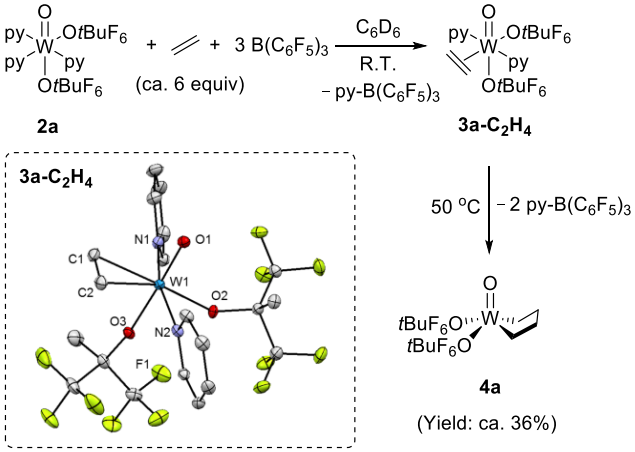

[a]Thermal ellipsoids plot at 50% probability; hydrogen atoms omitted. Yield of **4a** is determined by ^{1}H-NMR.

Reaction of **2a** with propylene leads to the formation of the propylene π complex **3a-C_3H_6** at room temperature. Its structure is confirmed by X-ray diffraction (Scheme 5). The major isomer of **3a-C_3H_6** shows carbon resonances at δ 24.4 (–CH_3), 66.0 (=CH_2) and 72.4 (=CH–) ppm. In the presence of 3 equiv of $B(C_6F_5)_3$, the py-$B(C_6F_5)_3$ adduct and **3a-C_3H_6** are formed together with ethylene and 2-butene as shown by in-situ ^{1}H-NMR studies (Figure S13). This result indicates that self-metathesis of propylene (ca. 6 equiv/[W]) occurs readily and reaches equilibrium in less than 15 min at room temperature.

Scheme 5. Reaction of 2a with propylene in the presence of $B(C_6F_5)_3$ and X-ray crystal structure of 3a-C_3H_6[a]

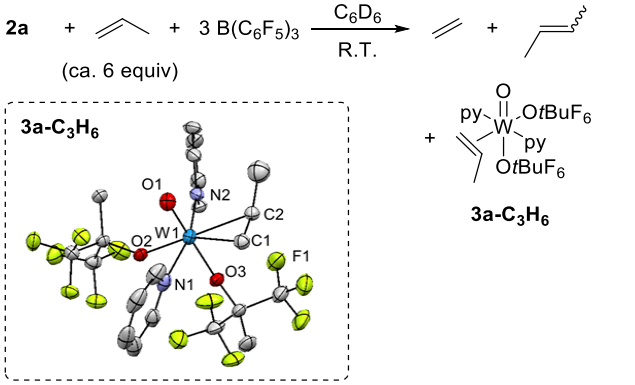

[a]Thermal ellipsoids plot at 50% probability; hydrogen atoms omitted.

Notably, the reaction of **2a** with styrene in the presence of 3 equiv of $B(C_6F_5)_3$ does not lead to the formation of self-metathesis products, even upon heating at 70 °C for 13 h, as shown by in-situ ^{1}H-NMR and GC-MS. In contrast, reaction of **2a**, $B(C_6F_5)_3$ and β-methylstyrene results in the formation of 2-butene and stilbene under the same conditions. The complex **2a** also reacts with allylbenzene in the presence of $B(C_6F_5)_3$ to form ethylene and 1,4-diphenyl-2-butene $PhCH_2(CH{=}CH)CH_2Ph$, in less than 45 min at room temperature (Scheme 6).

All these results suggest that the presence of an allylic C-H group is probably crucial for the conversion of the W(IV)-oxo pre-catalyst into the active species. In order to gain more insights into the initiation mechanism, we decided to conduct a detailed investigation of the reaction between **2a** and *trans*-β-

methylstyrene, in particular by monitoring the organic products formed during the activation period.

Scheme 6. Reactions of 2a with styrene, *β*-methylstyrene and allylbenzene in the presence of $B(C_6F_5)_3$

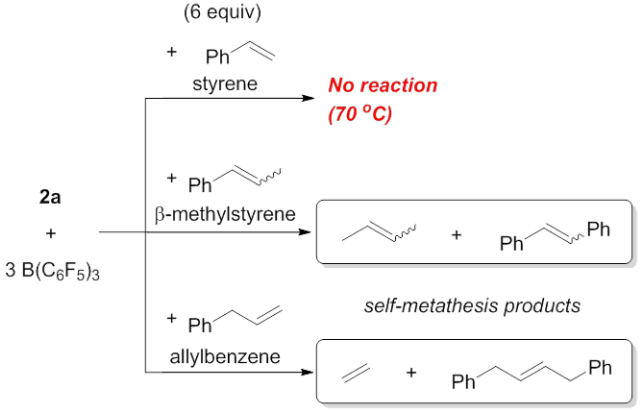

When monitoring the self-metathesis reaction of *trans*-*β*-methylstyrene (6 equiv/[W]) catalyzed by **2a** in the presence of $B(C_6F_5)_3$ (3 equiv/[W]), a small amount of styrene (0.05 equiv/[W]) is observed as a primary product according to GC-MS and no further formation is observed after ca. 30 min. In contrast, the formation of self-metathesis products is observed after a short induction period (Figure 1).

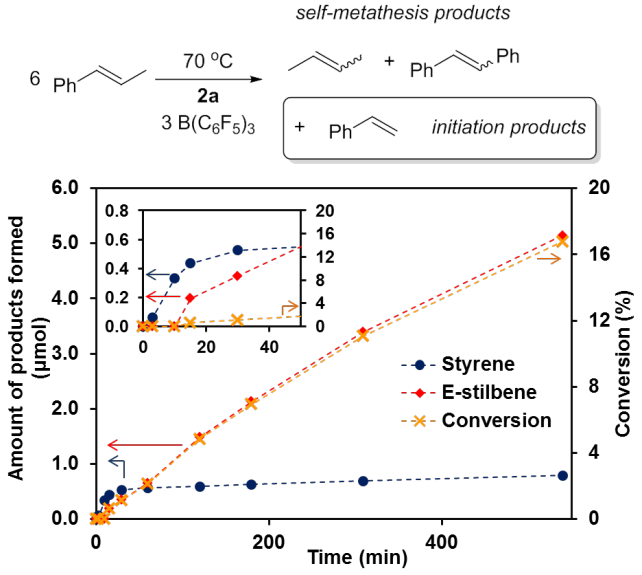

Figure 1. Formation of styrene (dark blue circle), *trans*-stilbene (red diamond) and conversion (orange cross) vs time plot at 70 °C.

These results support that styrene is an initiation product formed during the formation of the active alkylidene species. In addition, a small amount of propylene is observed in the gas phase by GC-FID implying the formation of a W-methylidene and its subsequent reaction with *trans*-*β*-methylstyrene or 2-butene. The observation of styrene as an initiation product points to the allyl hydride mechanism as the initiation step for alkylidene formation (Scheme 3). No other heavier organic product is observed suggesting that other initiation mechanisms are unlikely (Scheme S1). The observation of only a substoichiometric amount of styrene (0.05 equiv/[W]) suggests that only small amounts of active species are formed upon activation.

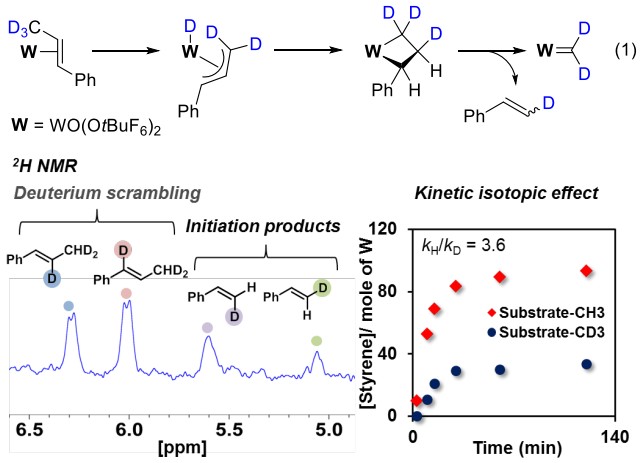

Figure 2. Left: ^{2}H-NMR spectrum at =CH region (for full spectrum, see Figure S17). Right: Concentration of styrene (normalized by the no. of mole of [W]) vs time plot with *trans*-*β*-methylstyrene (red diamond) and *trans*-*β*-(methyl-d_3)styrene (dark blue circle) as substrates.

In order to understand better how styrene is formed during the reaction and whether or not C-H activation is indeed an important elementary step in the initiation process, the reactivity of *trans*-*β*-(methyl-d_3)styrene with **2a** was also investigated. According to in-situ ^{2}H-NMR studies (Figure 2), *β*-deuteriostyrene is observed upon reaction of *trans*-*β*-(methyl-d_3)styrene and **2a** in the presence of 3 equiv of $B(C_6F_5)_3$. This observation further supports the proposed allyl hydride initiation mechanism (eq. 1). The initial rates of formation of initiation products with *trans*-*β*-(methyl-d_3)styrene and *trans*-*β*-methylstyrene show a k_H/k_D of 3.6 (Figure 2; see SI for details), a primary kinetic isotopic effect (KIE), which suggests the involvement of the allylic hydrogen atom in the rate-determining step.[45] Notably, the amount of styrene formed (0.01 equiv/[W]) upon using *trans*-*β*-(methyl-d_3)styrene is much lower than upon using *trans*-*β*-methylstyrene. The smaller amount of detected deuterated initiation product could be due to the slower rate of initiation for the deuterated alkene while decomposition could occur at similar rates for both deuterated and non-deuterated alkene during initiation. Such decomposition is likely one of the reasons for having intrinsically small amounts of active species. Even though the number of active species formed by using *trans*-*β*-(methyl-d_3)styrene is lower, the conversion of self-metathesis is slightly higher than that of *trans*-*β*-methylstyrene (Figure S19). This may be due to the advantageous isotope effect that can reduce deactivation via *β*-H elimination of the metathesis active metallacyclobutane intermediates.[40, 46-48]

Similarly, the reaction of **2a** with allylbenzene (6 equiv/[W]) in the presence of $B(C_6F_5)_3$ (3 equiv/[W]) also yields styrene which further supports the same allyl hydride intermediate. Meanwhile, isomerization of allylbenzene into the thermodynamically more stable *trans*-*β*-methylstyrene is also observed during this reaction. The observed double bond isomerization is known to possibly involve a *π*-allyl metal hydride intermediate.[49] Monitoring the reaction by in-situ ^{1}H-NMR indicates that the isomerization process occurs prior to metathesis (Figure S22). This result suggests that the formation of a metallacyclobutane from an allyl hydride is slower than the isomerization process.

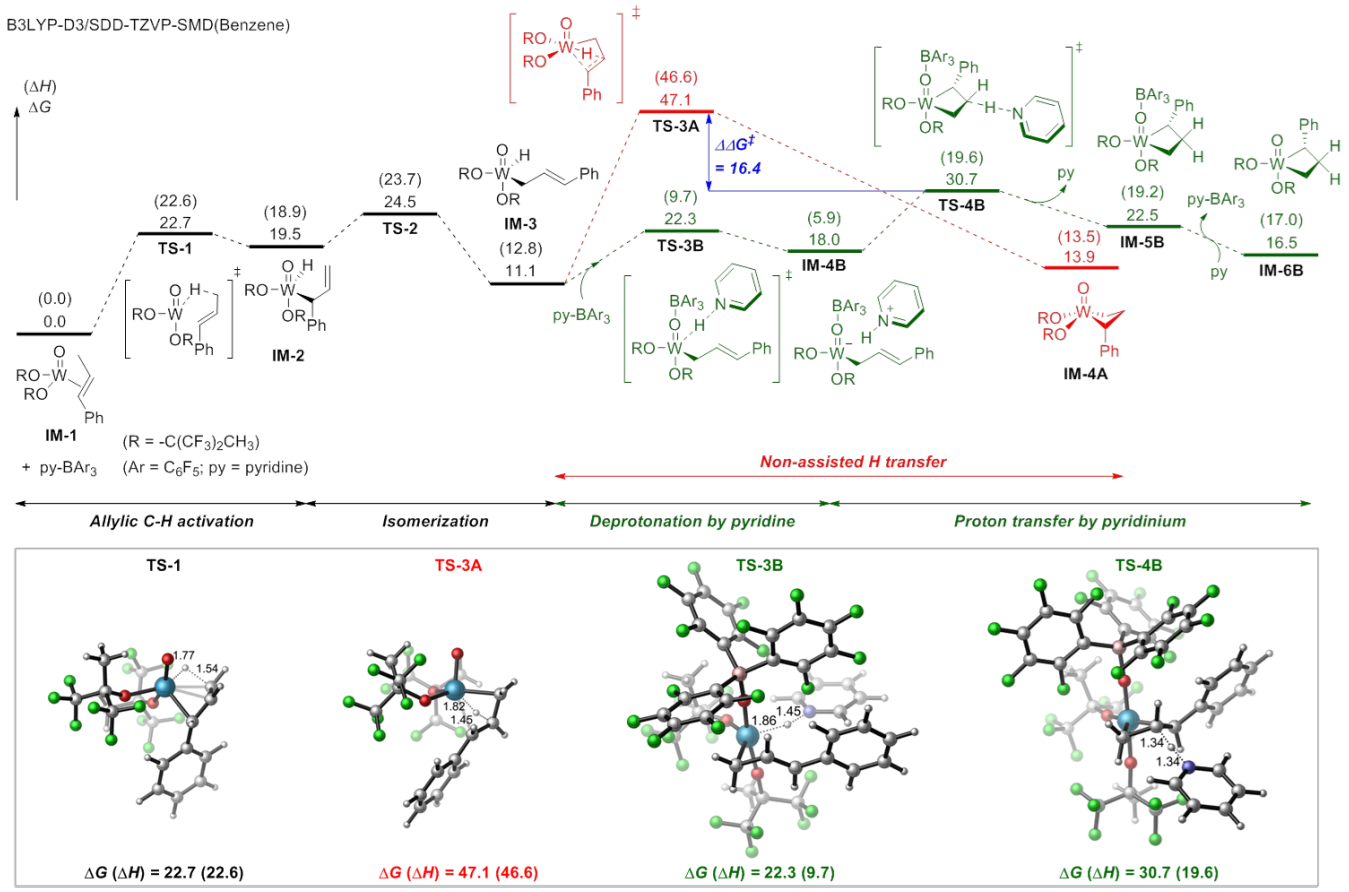

Figure 3. Computed Gibbs free energies and enthalpies in parentheses at 298.15 K (in kcal mol^{-1}) for initiation pathways via allyl hydride intermediates (Red: non-assisted; Green: assisted) involved in the reaction between **2a** and *trans*-*β*-methylstyrene (B3LYP-D3/SDD-TZVP-SMD(Benzene)).

To further probe the allylic C-H activation mechanism, DFT calculations were performed using **2a** and *trans*-*β*-methylstyrene in light of the kinetic findings mentioned above. The calculations show that formation of the pyridine free π complex (**IM-1**) is thermodynamically favorable in the presence of $B(C_6F_5)_3$ (Figure S42). The free energy barrier required for activating the allylic C-H bond (**TS-1**) to form W(VI) η^1-allyl hydride intermediate (**IM-2**) from the π complex (**IM-1**) is 22.7 kcal/mol (Figure 3). **IM-2** further converts into its isomer **IM-3** (ΔG = -8.4 kcal/mol). However, transferring the hydrogen atom to the *β*-carbon on the allyl group to form a metallacyclobutane requires a very high free energy barrier (**TS-3A**: $\Delta G^{\ddagger}$ = 36.0 kcal/mol with an overall barrier of $\Delta G^{\ddagger}$ = 47.1 kcal/mol), making this direct process unlikely. Since H-transfer is the most energy demanding step, we also consider additional factors that might play a role in facilitating this process. However, coordination of $B(C_6F_5)_3$ to the oxo ligand or $B(C_6F_5)_3$ assisted H-transfer are both high in energies (Figure S43). In particular, the free energy required for abstracting the H by $B(C_6F_5)_3$ is $\Delta G^{\ddagger}$ = 30.2 kcal/mol with an overall barrier of $\Delta G^{\ddagger}$ = 41.3 kcal/mol (**TS-3D**; Figure S43), suggesting that the H atom may not have a strong hydridic character and the subsequent formation of cationic W center is unfavorable.

Alternatively, pyridine can abstract the H from W to form an anionic π-allyl intermediate along with a pyridinium (PyH^+), which can then transfer the proton to the *β*-carbon of the allyl group and thus generate a metallacyclobutane. While the energy required for abstracting H by pyridine to form a pyridinium (PyH^+) intermediate is shown to be quite high ($\Delta G^{\ddagger}$ = 26.4 kcal/mol) (**TS-3E**; Figure S44), the energy barrier is significantly lowered (**TS-3B**: $\Delta G^{\ddagger}$ = 11.2 kcal/mol) upon coordination of $B(C_6F_5)_3$ onto the oxo ligand (Figure 3). This is likely facilitated by the decrease in electron density at the W center, and hence increasing the acidity of the "hydride" ligand. Furthermore, coordination of $B(C_6F_5)_3$ can also stabilize the anionic W center formed after H abstraction (**IM-4B** lies 18.0 kcal/mol above the reference state **IM-1**). While protonation of the *β*-carbon by PyH^+ (**TS-4B**) is the highest in energy for this pathway (overall energy barrier of $\Delta G^{\ddagger}$ = 30.7 kcal/mol), it lies significantly lower ($\Delta\Delta G^{\ddagger}$ = -16.4 kcal/mol) than **TS-3A** that corresponds to the non-assisted formation of metallacyclobutane. Note that the entropy and resulting free energy of activation for **TS-4B** is likely overestimated since it involves the dissociation and reaction of py-$B(C_6F_5)_3$ in solution (for detailed discussion see SI),[50] making this proton transfer step accessible. In fact, this step is similar to the recently reported reverse elementary step involved in the decomposition pathway of ruthenium metallacyclobutane induced by base.[51] Such proton transfer reactions (protonation or deprotonation) on the *β*-carbon are consistent with its formally positively charged nature as recently evidenced by detailed solid-state NMR analysis of trigonal bipyramidal metallacyclobutane intermediates.[31] In addition, the calculated KIE on this rate-determining proton transfer step (**TS-4B**) ($(k_H/k_D)_{DFT}$ = 3.7) matches well with the experimentally observed KIE ((k_H/k_D) = 3.6). The thus-formed metallacyclobutane (**IM-6B**)

can then undergo cycloreversion to give alkylidenes. The overall initiation process is endergonic by 10.8 and 13.6 kcal/mol with respect to the π complex **IM-1** (Figure S47) which explains the observation of only a small amount of initiation product and the difficulty to detect the propagating – alkylidenes and metallacyclobutanes – species by NMR. The small amounts of alkylidenes formed will participate in the catalytic conversion of β-methylstyrene into stilbene and 2-butene.

All the data above point to an initiation mechanism involving an allylic C-H activation by the W(IV) pre-catalyst. The thus-formed allyl hydride intermediate generates the required metallacyclobutane for metathesis by a proton transfer which is assisted by both pyridine and $B(C_6F_5)_3$. From this metallacyclobutane, cycloreversion yields a putative W(VI) alkylidene, which is active in metathesis, along with the olefinic initiation product. Both the observed primary KIE and the calculated highest energy transition state indicate that proton transfer is the rate-determining step in the activation process yielding metallacyclobutanes and alkylidenes (Scheme 7).

Scheme 7. Proposed initiation mechanism[a]

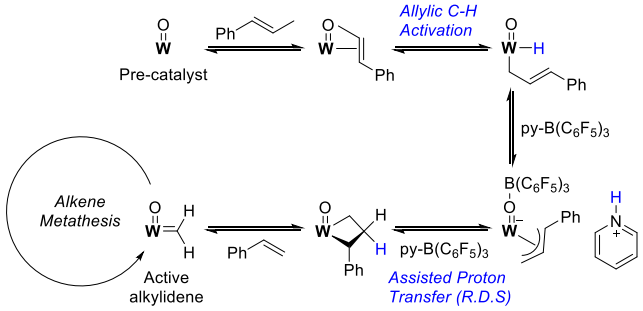

[a]**W** = W containing organometallic fragment

CONCLUSION

We have reported the first example of well-defined monomeric d^2 W(IV)-oxo bisalkoxide complexes that can initiate alkene metathesis and show comparable catalytic activities to W(VI)-oxo alkylidene complexes. Detailed studies of the initiation step including deuterium-labeling have shown that allylic C-H activation is involved during the activation of these W(IV) pre-catalysts. DFT computational studies reveal that both pyridine and $B(C_6F_5)_3$ are important for the formation of the metallacyclobutane, the initiation product and the metathesis activity. Our studies suggest that formation of the metallacyclobutane is the rate-determining initiation step, which involves a pyridine-assisted proton transfer to the β-carbon position of the allyl ligand and is consistent with the observed KIE. Based on the quantities of initiation products detected, the amounts of active intermediates (metallacyclobutane or alkylidene) formed are small, making direct spectroscopic observation of such intermediates a challenge. The small amounts of active intermediates are likely due to: i) the thermodynamically unfavorable initiation process and ii) competing decomposition of reactive intermediates during the initiation process. Nevertheless, the present work demonstrates the importance of assisted proton transfer pathways in generating alkylidene species and shows how a Lewis acid and Lewis base cooperate to generate the active species.[52] One may thus wonder if a similar pathway could also take place in the classical heterogeneous catalysts, where basic surface O atoms in combination with Lewis acids and strained surface sites could play a similar role. We are currently investigating this possibility.

ASSOCIATED CONTENT

Supporting Information. The Supporting Information is available free of charge on the ACS Publications website. Full experimental and computational details and catalytic data. (PDF)

AUTHOR INFORMATION

Corresponding Author

* ccoperet@ethz.ch

Funding Sources

The authors are grateful to the Swiss National Foundation (SNF) for financial support of this work (grant no. 200021L_157146) and to the French National Agency (ANR MASCAT, grant no. ANR-14-CE36-0010-01). This work was granted access to the HPC resources of TGCC and IDRIS under the allocation 2017-080609 made by GENCI.

ACKNOWLEDGMENT

Dr. Keith Searles is thanked for fruitful discussions. Christopher P. Gordon is thanked for providing NMR assistance.

REFERENCES

1. Grubbs, R. H.; Wenzel, A. G.; O'Leary, D. J.; Khosravi, E., *Handbook of Metathesis, 3 Vol. Set, 2nd ed.* Wiley VCH: Weinheim: 2015.
2. Grubbs, R. H.; Chang, S., Recent advances in olefin metathesis and its application in organic synthesis. *Tetrahedron* **1998,** *54*, 4413-4450.
3. Fürstner, A., Olefin Metathesis and Beyond. *Angew. Chem. Int. Ed.* **2000,** *39*, 3012-3043.
4. Schrock, R. R.; Hoveyda, A. H., Molybdenum and Tungsten Imido Alkylidene Complexes as Efficient Olefin-Metathesis Catalysts. *Angew. Chem. Int. Ed.* **2003,** *42*, 4592-4633.
5. Mol, J. C., Industrial applications of olefin metathesis. *J. Mol. Catal. A: Chem.* **2004,** *213*, 39-45.
6. Schrock, R. R., Multiple Metal–Carbon Bonds for Catalytic Metathesis Reactions (Nobel Lecture). *Angew. Chem. Int. Ed.* **2006,** *45*, 3748-3759.
7. Hoveyda, A. H.; Zhugralin, A. R., The remarkable metal-catalysed olefin metathesis reaction. *Nature* **2007,** *450*, 243.
8. Schrock, R. R., Recent Advances in High Oxidation State Mo and W Imido Alkylidene Chemistry. *Chem. Rev.* **2009,** *109*, 3211-3226.
9. Hoveyda, A. H.; Malcolmson, S. J.; Meek, S. J.; Zhugralin, A. R., Catalytic Enantioselective Olefin Metathesis in Natural Product Synthesis. Chiral Metal-Based Complexes that Deliver High Enantioselectivity and More. *Angew. Chem. Int. Ed.* **2009,** *49*, 34-44.
10. Higman, C. S.; Lummiss, J. A. M.; Fogg, D. E., Olefin Metathesis at the Dawn of Implementation in Pharmaceutical and Specialty-Chemicals Manufacturing. *Angew. Chem. Int. Ed.* **2016,** *55*, 3552-3565.
11. Nguyen, T. T.; Koh, M. J.; Shen, X.; Romiti, F.; Schrock, R. R.; Hoveyda, A. H., Kinetically controlled E-selective catalytic olefin metathesis. *Science* **2016,** *352*, 569.
12. Koh, M. J.; Nguyen, T. T.; Lam, J. K.; Torker, S.; Hyvl, J.; Schrock, R. R.; Hoveyda, A. H., Molybdenum chloride catalysts for Z-selective olefin metathesis reactions. *Nature* **2017,** *542*, 80.
13. Coperet, C.; Allouche, F.; Chan, K. W.; Conley, M. P.; Delley, M. F.; Fedorov, A.; Moroz, I. B.; Mougel, V.; Pucino, M.; Searles, K.; Yamamoto, K.; Zhizhko, P. A., Bridging the Gap between Industrial and Well-Defined Supported Catalysts. *Angew. Chem. Int. Ed.* **2018,** *57*, 6398-6440.

14. Lwin, S.; Wachs, I. E., Olefin Metathesis by Supported Metal Oxide Catalysts. *ACS Catal.* **2014,** *4*, 2505-2520.
15. Basrur, A. G.; Patwardhan, S. R.; Was, S. N., Propene metathesis over silica-supported tungsten oxide catalyst—Catalyst induction mechanism. *J. Catal.* **1991,** *127*, 86-95.
16. Ding, K.; Gulec, A.; Johnson, A. M.; Drake, T. L.; Wu, W.; Lin, Y.; Weitz, E.; Marks, L. D.; Stair, P. C., Highly Efficient Activation, Regeneration, and Active Site Identification of Oxide-Based Olefin Metathesis Catalysts. *ACS Catal.* **2016,** *6*, 5740-5746.
17. Howell, J. G.; Li, Y.-P.; Bell, A. T., Propene Metathesis over Supported Tungsten Oxide Catalysts: A Study of Active Site Formation. *ACS Catal.* **2016,** *6*, 7728-7738.
18. Lwin, S.; Li, Y.; Frenkel, A. I.; Wachs, I. E., Nature of WOx Sites on SiO_2 and Their Molecular Structure–Reactivity/Selectivity Relationships for Propylene Metathesis. *ACS Catal.* **2016,** *6*, 3061-3071.
19. Lwin, S.; Wachs, I. E., Catalyst Activation and Kinetics for Propylene Metathesis by Supported WOx/SiO_2 Catalysts. *ACS Catal.* **2017,** *7*, 573-580.
20. Amakawa, K.; Wrabetz, S.; Kröhnert, J.; Tzolova-Müller, G.; Schlögl, R.; Trunschke, A., In Situ Generation of Active Sites in Olefin Metathesis. *J. Am. Chem. Soc.* **2012,** *134*, 11462-11473.
21. Amakawa, K.; Sun, L.; Guo, C.; Hävecker, M.; Kube, P.; Wachs, I. E.; Lwin, S.; Frenkel, A. I.; Patlolla, A.; Hermann, K.; Schlögl, R.; Trunschke, A., How Strain Affects the Reactivity of Surface Metal Oxide Catalysts. *Angew. Chem. Int. Ed.* **2013,** *52*, 13553-13557.
22. Chakrabarti, A.; Wachs, I. E., Molecular Structure–Reactivity Relationships for Olefin Metathesis by Al2O3-Supported Surface MoOx Sites. *ACS Catal.* **2018,** *8*, 949-959.
23. Mougel, V.; Chan, K.-W.; Siddiqi, G.; Kawakita, K.; Nagae, H.; Tsurugi, H.; Mashima, K.; Safonova, O.; Copéret, C., Low Temperature Activation of Supported Metathesis Catalysts by Organosilicon Reducing Agents. *ACS Cent. Sci.* **2016,** *2*, 569-576.
24. Yamamoto, K.; Chan, K. W.; Mougel, V.; Nagae, H.; Tsurugi, H.; Safonova, O. V.; Mashima, K.; Coperet, C., Silica-supported isolated molybdenum di-oxo species: formation and activation with organosilicon agent for olefin metathesis. *Chem. Commun.* **2018,** *54*, 3989-3992.
25. Schrock, R. R.; Lopez, L. P. H.; Hafer, J.; Singh, R.; Sinha, A.; Müller, P., Olefin Metathesis Reactions Initiated by d2 Molybdenum or Tungsten Complexes. *Organometallics* **2005,** *24*, 5211-5213.
26. Marinescu, S. C.; King, A. J.; Schrock, R. R.; Singh, R.; Müller, P.; Takase, M. K., Simple Molybdenum(IV) Olefin Complexes of the Type Mo(NR)(X)(Y)(olefin). *Organometallics* **2010,** *29*, 6816-6828.
27. de la Mata, F. J.; Grubbs, R. H., Synthesis and Reactions of Tungsten Oxo Vinylalkylidene Complexes: Reactions of WCl2(O)(PX3) (X = OMe, R) Precursors with 3,3-Diphenylcyclopropene. *Organometallics* **1996,** *15*, 577-584.
28. Javier de la Mata, F., Synthesis and characterization of tungsten oxo alkylidene complexes via the reaction of WCl2(O)[PX3]3 (PX3 = $P(OMe)_3$, PMe_2Ph, $PMePh_2$) with 4,8-dioxaspiro[2,5]oct-1-ene (ketalcyclopropene). *J. Organomet. Chem.* **1996,** *525*, 183-189.
29. Peryshkov, D. V.; Forrest, W. P.; Schrock, R. R.; Smith, S. J.; Müller, P., $B(C_6F_5)_3$ Activation of Oxo Tungsten Complexes That Are Relevant to Olefin Metathesis. *Organometallics* **2013,** *32*, 5256-5259.
30. Hock, A. S.; Schrock, R. R.; Hoveyda, A. H., Dipyrrolyl Precursors to Bisalkoxide Molybdenum Olefin Metathesis Catalysts. *J. Am. Chem. Soc.* **2006,** *128*, 16373-16375.
31. Gordon, C. P.; Yamamoto, K.; Liao, W.-C.; Allouche, F.; Andersen, R. A.; Copéret, C.; Raynaud, C.; Eisenstein, O., Metathesis Activity Encoded in the Metallacyclobutane Carbon-13 NMR Chemical Shift Tensors. *ACS Cent. Sci.* **2017,** *3*, 759-768.
32. Peryshkov, D. V.; Schrock, R. R.; Takase, M. K.; Müller, P.; Hoveyda, A. H., Z-Selective Olefin Metathesis Reactions Promoted by Tungsten Oxo Alkylidene Complexes. *J. Am. Chem. Soc.* **2011,** *133*, 20754-20757.
33. Peryshkov, D. V.; Schrock, R. R., Synthesis of Tungsten Oxo Alkylidene Complexes. *Organometallics* **2012,** *31*, 7278-7286.
34. Conley, M. P.; Mougel, V.; Peryshkov, D. V.; Forrest, W. P.; Gajan, D.; Lesage, A.; Emsley, L.; Copéret, C.; Schrock, R. R., A Well-Defined Silica-Supported Tungsten Oxo Alkylidene Is a Highly Active Alkene Metathesis Catalyst. *J. Am. Chem. Soc.* **2013,** *135*, 19068-19070.
35. Mougel, V.; Copéret, C., Isostructural Molecular and Surface Mimics of the Active Sites of the Industrial WO_3/SiO_2 Metathesis Catalysts. *ACS Catal.* **2015,** *5*, 6436-6439.
36. Schowner, R.; Frey, W.; Buchmeiser, M. R., Cationic Tungsten-Oxo-Alkylidene-N-Heterocyclic Carbene Complexes: Highly Active Olefin Metathesis Catalysts. *J. Am. Chem. Soc.* **2015,** *137*, 6188-6191.
37. Schrock, R. R.; Copéret, C., Formation of High-Oxidation-State Metal–Carbon Double Bonds. *Organometallics* **2017,** *36*, 1884-1892.
38. Schrock, R. R.; Duval-Lungulescu, M.; Tsang, W. C. P.; Hoveyda, A. H., Catalytic Homologation of Vinyltributylstannane to Allyltributylstannane by Mo(IV) Complexes in the Presence of Ethylene. *J. Am. Chem. Soc.* **2004,** *126*, 1948-1949.
39. McLain, S. J.; Sancho, J.; Schrock, R. R., Metallacyclopentane to metallacyclobutane ring contraction. *J. Am. Chem. Soc.* **1979,** *101*, 5451-5453.
40. Tsang, W. C. P.; Hultzsch, K. C.; Alexander, J. B.; Bonitatebus, P. J.; Schrock, R. R.; Hoveyda, A. H., Alkylidene and Metalacyclic Complexes of Tungsten that Contain a Chiral Biphenoxide Ligand. Synthesis, Asymmetric Ring-Closing Metathesis, and Mechanistic Investigations. *J. Am. Chem. Soc.* **2003,** *125*, 2652-2666.
41. Wang, S.-Y. S.; VanderLende, D. D.; Abboud, K. A.; Boncella, J. M., Metallacyclopentane Formation: A Deactivation Pathway for a Tungsten(VI) Alkylidene Complex in Olefin Metathesis Reactions. *Organometallics* **1998,** *17*, 2628-2635.
42. Tsang, W. C. P.; Jamieson, J. Y.; Aeilts, S. L.; Hultzsch, K. C.; Schrock, R. R.; Hoveyda, A. H., Investigations of Reactions between Chiral Molybdenum Imido Alkylidene Complexes and Ethylene: Observation of Unsolvated Base-Free Methylene Complexes, Metalacyclobutane and Metalacyclopentane Complexes, and Molybdenum(IV) Olefin Complexes. *Organometallics* **2004,** *23*, 1997-2007.
43. Robbins, J.; Bazan, G. C.; Murdzek, J. S.; O'Regan, M. B.; Schrock, R. R., Reduction of molybdenum imido-alkylidene complexes in the presence of olefins to give molybdenum(IV) complexes. *Organometallics* **1991,** *10*, 2902-2907.
44. Fellmann, J. D.; Rupprecht, G. A.; Schrock, R. R., Rapid selective dimerization of ethylene to 1-butene by a tantalum catalyst and a new mechanism for ethylene oligomerization. *J. Am. Chem. Soc.* **1979,** *101*, 5099-5101.
45. Simmons, E. M.; Hartwig, J. F., On the Interpretation of Deuterium Kinetic Isotope Effects in C-H Bond Functionalizations by Transition-Metal Complexes. *Angew. Chem. Int. Ed.* **2012,** *51*, 3066-3072.
46. Arndt, S.; Schrock, R. R.; Müller, P., Synthesis and Reactions of Tungsten Alkylidene Complexes That Contain the 2,6-Dichlorophenylimido Ligand. *Organometallics* **2007,** *26*, 1279-1290.
47. Solans-Monfort, X.; Coperet, C.; Eisenstein, O., Shutting Down Secondary Reaction Pathways: The Essential Role of the Pyrrolyl Ligand in Improving Silica Supported d^0-ML4 Alkene Metathesis Catalysts from DFT Calculations. *J. Am. Chem. Soc.* **2010,** *132*, 7750-7757.
48. Solans-Monfort, X.; Copéret, C.; Eisenstein, O., Oxo vs Imido Alkylidene d^0-Metal Species: How and Why Do They Differ in Structure, Activity, and Efficiency in Alkene Metathesis? *Organometallics* **2012,** *31*, 6812-6822.
49. Larionov, E.; Li, H.; Mazet, C., Well-defined transition metal hydrides in catalytic isomerizations. *Chem. Commun.* **2014,** *50*, 9816-9826.
50. For recent discussion on computing entropies see reference below: [a] Besora, M.; Vidossich, P.; Lledós, A.; Ujaque, G.; Maseras, F., Calculation of Reaction Free Energies in Solution: A Comparison of Current Approaches. *J. Phys. Chem. A* **2018,** *122*, 1392-1399.; [b] Falivene, L.; Barone, V.; Talarico, G., Unraveling the role of entropy

in tuning unimolecular vs. bimolecular reaction rates: The case of olefin polymerization catalyzed by transition metals. *Mol. Catal.* **2018,** *452*, 138-144.
51. Bailey, G. A.; Lummiss, J. A. M.; Foscato, M.; Occhipinti, G.; McDonald, R.; Jensen, V. R.; Fogg, D. E., Decomposition of Olefin Metathesis Catalysts by Brønsted Base: Metallacyclobutane Deprotonation as a Primary Deactivating Event. *J. Am. Chem. Soc.* **2017,** *139*, 16446-16449.
52. Stephan, D. W.; Erker, G., Frustrated Lewis Pair Chemistry: Development and Perspectives. *Angew. Chem. Int. Ed.* **2015,** *54*, 6400-6441.

TOC

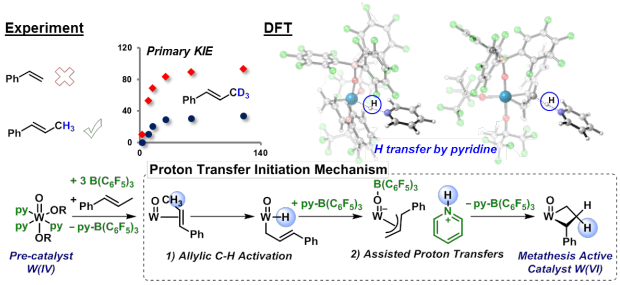
Experiment
DFT
Primary KIE
120
80
40
0
0
140
Ph
CD3
CH3
H transfer by pyridine
Proton Transfer Initiation Mechanism
+ 3 B(C6F5)3
+ Ph
– py-B(C6F5)3
+ py-B(C6F5)3
– py-B(C6F5)3
Pre-catalyst W(IV)
1) Allylic C-H Activation
2) Assisted Proton Transfers
Metathesis Active Catalyst W(VI)